

Full Paper

New Quinoline Derivatives as Sulfuric Acid Inhibitor's for Mild Steel

Nadia Dkhireche,¹ Mouhsine Galai,¹ Younes El Kacimi,^{1,*} Mohamed Rbaa,² Moussa Ouakki,³ Brahim Lakhrissi² and Mohammed Ebn Touhami¹

¹*Laboratory of Materials Engineering and Environment: Modeling and Application, Faculty of Science, University Ibn Tofail BP. 133-14000, Kenitra, Morocco*

²*Laboratoire d'Agroressources et Génie des Procédés, Faculté des Sciences, Faculty of Science, Ibn Tofail University, Kénitra, Morocco*

³*Laboratory of Materials, Electrochemistry and Environment, Faculty of Science, Ibn Tofail University, Kénitra, Morocco*

*Corresponding Author, Tel.: +212663566545

E-Mail: elkacimiyounes@yahoo.fr

Received: 4 July 2017 / Received in revised form: 14 October 2017 /

Accepted: 31 October 2017 / Published online: 31 January 2018

Abstract- Two newly synthesised Quinoline derivatives, namely 5-((2-(4-dimethylamino)phenyl)-1H-benzo[d]imidazol-1-yl)methyl)quinolin-8-ol (*Q-N(CH₃)₂*) and 5-((2-(4-nitrophenyl)-1H-benzo[d]imidazol-1-yl)methyl)quinolin-8-ol (*Q-NO₂*) were studied as inhibitors for the corrosion of mild steel in 0.5 M sulphuric acid solution has been examined and characterized by weight loss, polarization and electrochemical impedance spectroscopy (EIS). The experimental results reveal that the organic compound has a good inhibiting effect on the mild steel in 0.5 M H₂SO₄ solution. The protection efficiency increases with increasing inhibitor concentration, but the temperature has hardly effect on the inhibition efficiency of *Q-N(CH₃)₂* and *Q-NO₂*. The adsorption of the inhibitors on the surface of mild steel in a 0.5 M H₂SO₄ solution was found to obey Langmuir's adsorption isotherm. Thermodynamic data clearly show that the adsorption mechanism of *Q-N(CH₃)₂* and *Q-NO₂* on mild steel surface in 0.5 M H₂SO₄ solution is mainly electrostatic-adsorption. Potentiodynamic polarization studies have shown that Quinoline derivatives acts as a mixed type of inhibitor. Data obtained from EIS studies were analyzed to model inhibition process through appropriate equivalent circuit model. The Scanning Electron Microscope (SEM) images of the corrosion product confirmed the protection offered by the extract on the surface of the metal immersed in both media.

Keywords- Quinoline derivatives, Corrosion inhibition, Mild steel, Sulphuric Acid, EIS

1. INTRODUCTION

Iron and its alloys used in industrial sectors became a great challenge for corrosion engineers or scientists. So, to remove the scale and other products from the metal working, cleaning of boilers and heat exchangers, the acid solutions are commonly used. In these cases the metals were damaged by corrosion phenomena. Thus, to minimize this problem, many inhibitors are used. In addition, organic compounds have many advantages such as high inhibition efficiency, low price, and easy production [1,3].

The search for new and efficient corrosion inhibitors becomes an obligation to secure metallic materials against corrosion. The effectiveness of organic compounds containing heteroatoms as corrosion inhibitors for steels in sulfuric acid is well developed [4–9].

The adsorption of inhibitors takes place through heteroatoms such as nitrogen, oxygen, phosphorus and sulfur, triple bonds or aromatic rings. The nature of heteroatom and substituents plays the major role in adsorption phenomenon. Also the existing data show that most organic inhibitors adsorb on the metal surface by displacing water molecules on the surface and forming a compact barrier film [10,11]. These compounds inhibit corrosion by adsorbing on metallic surface using heteroatoms (e.g. N, O, S), polar functional groups (e.g. -OH, -NH₂, -NO₂, -CN etc.), pi-electrons and aromatic rings as adsorption centers [12,13].

Recently many workers have reoriented their attention to the development of new corrosion inhibitors based on organic compounds such as pyrazole [14–16], triazole [17–22], tetrazole [23,24], phenyltetrazole [1,25], quinolinol [26], quinoline [27], imidazole [28–30] and oxadiazole derivatives [31–34]. The corrosion inhibition efficiency of organic compounds is related to their adsorption properties. Studies report that the adsorption of organic inhibitors mainly depends on some physicochemical properties of the molecule, related to its functional groups, to the possible steric effects and electronic density of donor atoms. Adsorption is supposed also to depend on the possible interaction of *p*-orbitals of the inhibitor with *d*-orbitals of the surface atoms, which induces greater adsorption of the inhibitor molecules onto the surface of mild steel, leading to the formation of a corrosion protecting film.

Thermodynamic parameters such as adsorption heat, adsorption entropy and adsorption free energy can be obtained from experimental data of the studies of the inhibition process at different temperatures. The kinetic data such as apparent activation energy and pre-exponential factor at different inhibitor concentrations are calculated, and the effects of the activation energy and pre-exponential factor on the corrosion rate of steel were discussed [35–39]. The inhibition action is satisfactorily explained by using both thermodynamic and kinetic models.

We have reported in a recent study the effect of new quinoline derivatives in the corrosion of steel in hydrochloric acid [27]. The presence of -N(CH₃)₂ group or -NO₂ group in some quinoline derivatives increased the inhibition efficiency. In continuation of this work,

we report the results of our evaluation of the tested quinoline derivatives, namely 5-((2-(4-dimethylamino)phenyl)-1H-benzo[d]imidazol-1-yl)methyl)quinolin-8-ol ($Q-N(CH_3)_2$) and 5-((2-(4-nitrophenyl)-1H-benzo[d]imidazol-1-yl)methyl)quinolin-8-ol ($Q-NO_2$), as corrosion inhibitors for mild steel in 0.5 M H_2SO_4 and its comparison with previous work in 1.0 M HCl medium. In the following, we present experimental data obtained by gravimetric measurements, potentiodynamic polarization curves, and electrochemical impedance spectroscopy. It is also aimed to predict the thermodynamic feasibility of quinoline adsorption on the metallic surface. In addition, detailed investigations of temperature on the system's electrochemical parameters were also studied and discussed to improve understanding of the adsorption mechanism of the studied inhibitors.

2. EXPERIMENTAL SECTION

2.1. Material preparation

The molecular formulas of the examined inhibitors are shown in Fig. 1. Their concentrations range were from 10^{-6} M to 10^{-3} M. Corrosion tests were performed on a mild steel with percentage composition as follows (wt%): 0.09% P; 0.38% Si; 0.01% Al; 0.05% Mn; 0.21% C; 0.05% S; and remainder Fe.

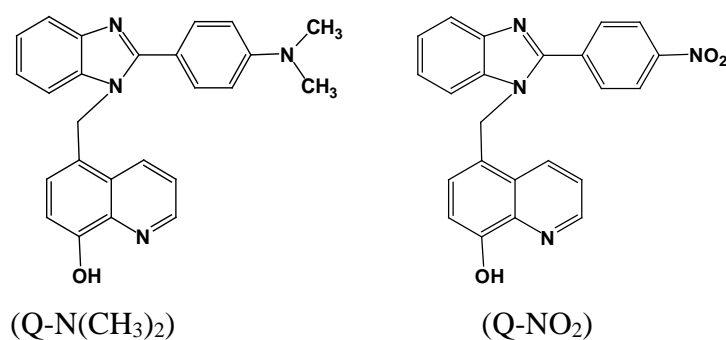


Fig. 1. Chemical structures of inhibitors, ($Q-N(CH_3)_2$) 5-((2-(4-dimethylamino)phenyl)-1H-benzo[d]imidazol-1-yl)methyl)quinolin-8-ol and ($Q-NO_2$) 5-((2-(4-nitrophenyl)-1H-benzo[d]imidazol-1-yl)methyl)quinolin-8-ol

Prior to the immersion test, the surface of the specimens was abraded using emery paper up to 1,200 grade, cleaned with acetone, washed with distilled water, and finally dried. The aggressive solution of 0.5 M H_2SO_4 was prepared by dilution of analytical grade 95–97% H_2SO_4 with distilled water.

2.2. Weight loss measurements

Weight loss experiments were done according to ASTM methods described previously [40,41]. Tests were conducted in 0.5 M of H₂SO₄ at 298±2 K. Gravimetric measurements were carried out in an electrolysis cell equipped with a thermostat-cooling condenser. The mild steel specimens used have a rectangular form 2.5 cm×2.0 cm×0.05 cm. After immersion period, the specimens were cleaned according to ASTM G-81 and reweighed to 10⁻⁴ g for determining corrosion rate [41]. Duplicate experiments are performed in each case, and the mean value of the weight loss is reported. Weight loss allows us to calculate the mean corrosion rate as expressed in (mg cm⁻² h⁻¹), either by chemical analysis of dissolved metal in solution or by gravimetric method measuring. The resulting quantity, corrosion rate (ω_{corr}) is there by the fundamental measurement in corrosion. (ω_{corr}) can be determined weight of specimen before and after exposure in the aggressive solution applying the following equation 1:

$$\omega_{corr} = \frac{m_i - m_f}{S \times t} \quad (1)$$

Where m_i , m_f , S and t de note initial weight, final weight, surface of specimen and immersion time, respectively.

The inhibition efficiency, $\eta_{\omega}\%$, is determined as follows:

$$\eta_{\omega} (\%) = \frac{\omega_{corr}^0 - \omega_{corr}}{\omega_{corr}^0} \times 100 \quad (2)$$

Where ω_{corr}^0 and ω_{corr} are the corrosion rates in the absence and presence of inhibitors, respectively.

2.3. Potentiodynamic polarization measurements

The working electrode was immersed in the test solution until the steady state corrosion potential (E_{corr}) was obtained. The anodic and cathodic polarization curves were recorded by polarization from a negative direction to a positive direction with the potential sweep rate equal to 1 mV/s using a VoltaLab PGZ 100 (Radiometer Analytical), monitored by a personal computer. The evaluation of corrosion kinetics parameters was obtained using a non-linear regression calculation according to Stern–Geary equation:

$$i = i_a + i_c = i_{corr} \left\{ \exp \left[b_a \times (E - E_{corr}) \right] - \exp \left[b_c \times (E - E_{corr}) \right] \right\} \quad (3)$$

Where i_{corr} is the corrosion current density ($A\ cm^{-2}$), b_a and b_c are the Tafel constants of anodic and cathodic reactions (V^{-1}), respectively. These constants are linked to the Tafel slopes β (V/dec) in usual logarithmic scale given by equation (4):

$$\beta = \frac{\ln 10}{b} = \frac{2.303}{b} \quad (4)$$

The corrosion parameters were then evaluated by means of nonlinear least square method by applying equation (2) using Origin software. However, for this calculation, the potential range applied was limited to ± 0.100 V around E_{corr} , else a significant systematic divergence was sometimes observed for both anodic and cathodic branches.

The corrosion inhibition efficiency is evaluated from the corrosion current densities values using the relationship (5):

$$\eta_{PP} = \frac{i_{corr}^0 - i_{corr}}{i_{corr}^0} \times 100 \quad (5)$$

The surface coverage values (θ) have been obtained from polarization curves for various concentrations of inhibitor using the following equation [42]:

$$\theta = 1 - \frac{i_{corr}}{i_{corr}^0} \quad (6)$$

Where i_{corr}^0 and i_{corr} are the corrosion current densities values without and with inhibitor, respectively.

2.4. EIS measurements

The electrochemical impedance spectroscopy measurements were carried out using a transfer function analyzer (VoltaLab PGZ 100), with a small amplitude a.c. signal (10 mV rms), over a frequency domain from 100 kHz to 100 mHz with five points per decade. The EIS diagrams were done in the Nyquist representation. The results were then analyzed in terms of an equivalent electrical circuit using Boukamp program [43].

The inhibiting efficiency derived from EIS, η_{EIS} is also added in Table 3 and calculated using the following equation (7):

$$\eta_{EIS} = \frac{R_{ct} - R_{ct}^0}{R_{ct}} \times 100 \quad (7)$$

Where R_{ct}^0 and R_{ct} are the charge transfer resistance values in the absence and in the presence of inhibitor, respectively.

In order to ensure reproducibility, all experiments were repeated three times. The evaluated inaccuracy did not exceed 10%.

2.5. Scanning Electron Microscope Characterization (SEM)

The morphological changes over the mild steel surfaces in absence and presence of Q-(CH₃)₂ and Q-NO₂ compounds were analyzed by Scanning Electron Microscope Characterization (SEM). Here the specimens were immersed in 0.5 M H₂SO₄ in absence and presence of optimum concentration (10⁻³ M) of inhibitors for 6 h, respectively, then taken out from the test solutions, cleaned with bi-distilled water and dried it.

3. RESULTS AND DISCUSSION

3.1. Comparative study in 1.0 M HCl and 0.5 M H₂SO₄

The addition effect of Q-N(CH₃)₂ and Q-NO₂ at different concentrations on mild steel corrosion in 0.5 M H₂SO₄ solutions was studied by weight loss at 298±2 K after 12 h of immersion. The calculated values of corrosion rate (ω_{corr}) and E(%) are given in Table 1.

Corrosion rate decreases with increase in inhibitor concentration while E(%) values increase with increase in quinolines derivatives compounds concentration (Table 1). The inhibition efficiencies in the case of hydrochloric acid show the same trend as those previously obtained from AC impedance studies [27].

At the highest inhibitor concentration, 10⁻³ M, the maximum values of inhibition efficiency is 95.2% for Q-N(CH₃)₂ and 82.0% for Q-NO₂ were obtained in 1.0 M HCl solution. In the case of H₂SO₄, a small deviation of $E_{\omega}(\%)$ was observed. The results obtained is 93.6% for Q-N(CH₃)₂ and 92.3% for Q-NO₂ (Table 1). This result is best explained in terms of adsorbability of Cl⁻ and SO₄²⁻ [44].

Adsorption of organic molecules is not always a direct combination of the organic molecules with the metal surface [45]. In some cases, the adsorption occurs through the already adsorbed chloride or sulphate ions which interfere with the adsorbed organic molecules [46]. Indeed, the specific adsorption of anions is expected to be more pronounced with anions having a smaller degree of hydration, such as chloride ions. Being specifically adsorbed, they create an excess of negative charge towards the solution phase and favour more adsorption of quinoline derivatives compounds, leading to greater inhibition [47].

It is demonstrated during this study that these compounds are good inhibitor's for mild steel corrosion in 1.0 M HCl and 0.5 H₂SO₄ solution which.

In order to confirm the best protective properties of 5-((X-1H-benzo[d]imidazol-1-yl)-methyl)quinolin-8-ol (X : -N(CH₃)₂ and -NO₂) in 0.5 M H₂SO₄ medium, the effect of concentration, temperature and immersion time, was investigated using ac and dc electrochemical techniques.

3.2. Effect of concentration sulfuric acid inhibitor's

3.2.1. Weight loss measurements

The effect of different concentration of substituted quinoline compounds on the inhibition of mild steel corrosion in 0.5 M H₂SO₄ was studied using gravimetric method due to its simplicity and good reliability.

Table 1. Corrosion parameters obtained from weight loss and electrochemical measurements of mild steel in 0.5 M H₂SO₄ without and with different concentrations of Q-N(CH₃)₂ and Q-NO₂

Inhibitor Conc. / M	Weight loss		Polarisation curves					
	ω_{corr} (mg cm ⁻² h ⁻¹)	η_{ω} %	E_{corr} (mV/SCE)	i_{corr} (μ A cm ⁻²)	Tafel plot (mV dec ⁻¹)		η_{pp} %	θ
					$-\beta_c$	β_a		
0	1.53	-	-451	1850	-90	144	-	-
Q-N(CH ₃) ₂ / 0.5 M of H ₂ SO ₄ / Mild steel								
10 ⁻⁶	0.86	43.8	-458	1014	-125	97	43.7	0.44
10 ⁻⁵	0.62	59.5	-489	920	-118	111	50.3	0.50
10 ⁻⁴	0.16	89.5	-480	183	-115	114	90.1	0.90
10 ⁻³	0.12	92.2	-500	118	-84	115	93.6	0.94
Q-N(CH ₃) ₂ / 1.0 M of HCl / Mild steel [27]								
10 ⁻⁶	9.20	76.4	494	226	-86	90	77.0	494
10 ⁻⁵	6.01	84.6	475	135	-90	88	86.3	475
10 ⁻⁴	3.89	90.1	496	77	-106	99	92.2	496
10 ⁻³	2.67	93.1	482	47	-96	92	95.2	482
Q-NO ₂ / 0.5 M of H ₂ SO ₄ / Mild steel								
10 ⁻⁶	0.79	48.4	-452	1040	-126	103	43.7	0.44
10 ⁻⁵	0.56	63.4	-451	680	-120	84	63.0	0.63
10 ⁻⁴	0.31	79.7	-461	394	-112	111	79.0	0.79
10 ⁻³	0.14	90.8	-483	154	-102	120	92.3	0.92
Q-NO ₂ / 1.0 M of HCl / Mild steel [27]								
10 ⁻⁶	32.70	32.7	484	644	-153	78	34.5	484
10 ⁻⁵	19.20	50.7	513	490	-85	66	50.2	513
10 ⁻⁴	18.01	53.7	504	450	-87	62	54.3	504
10 ⁻³	6.67	82.9	499	179	-84	73	82.0	499

The observed weight-loss values of triplicate measurements are highly reproducible giving standard deviations. The inhibition efficiency (η_{ω} %) and other parameters such as corrosion rate (ω_{corr}) and surface coverage (θ) at various concentration of the inhibitors are given in Table 1. Careful examination of the results showed that protection efficiencies of the studied inhibitors increase with increasing concentrations. Maximum values of (inhibition efficiency) 92.2% for Q-N(CH₃)₂ and 90.8% for Q-NO₂ were obtained at 10⁻³ M. It has been reported that at lower concentrations, inhibitors preferably adsorb by flat orientation such that

as the concentration increases, surface coverage and consequently inhibition efficiency increases. However, if the concentration of the inhibitor is increased beyond certain (optimum) value, the inhibitor molecules adsorb perpendicularly onto the metallic surface due to electrostatic repulsion between the molecules at higher concentration. Therefore, after the optimum concentration of the inhibitor, the inhibition performance does not change significantly.

The order of inhibition efficiencies in Table 1 is $Q-N(CH_3)_2 > Q-NO_2$. The high inhibition efficiency of $Q-N(CH_3)_2$ compared to $Q-NO_2$ is due to the presence of electron donating ($-CH_3$) group in $Q-N(CH_3)_2$ there by enhances its ability to donate charges to the metal during the adsorption process.

3.2.2. Open circuit potential (OCP) measurements

The variances of OCP of the mild steel as a function of time in aerated 0.5 M H_2SO_4 solution, in the absence and presence of different concentrations of $Q-N(CH_3)_2$ and $Q-NO_2$ are shown in Fig. 1 and 2 respectively.

It was noticed that the addition of the inhibitors molecules induces a continuous shift in OCP (i.e., E_{corr}) to nobler potentials, indicating the spontaneous adsorption of inhibitor onto the metallic surface.

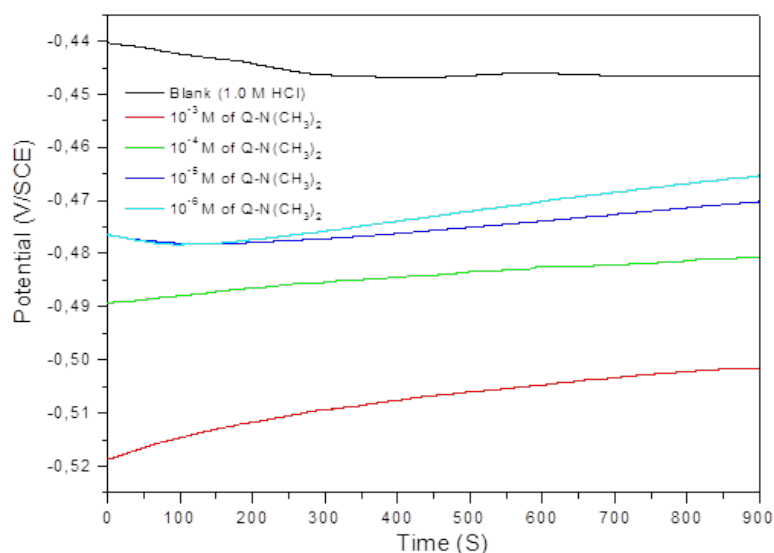


Fig. 1. OCP vs. time for mild steel in 0.5 M H_2SO_4 without and with $Q-N(CH_3)_2$

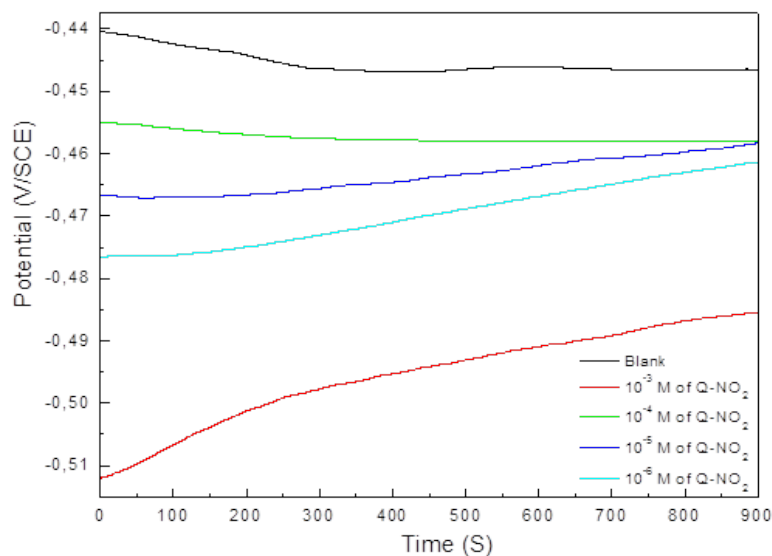


Fig. 2. OCP vs. time for mild steel in 0.5 M H₂SO₄, without and with Q-NO₂

3.2.3. Potentiodynamic polarization curves

Polarisation curves of the mild steel electrode in 0.5 M H₂SO₄ without and with addition of Q-N(CH₃)₂ and Q-NO₂ at different concentrations are shown in Fig. 3 and 4 respectively. As it can be seen, both cathodic and anodic reactions of mild steel electrode corrosion were inhibited by the increase of quinoline derivatives concentration in 0.5 M H₂SO₄. Q-N(CH₃)₂ and Q-NO₂ suppressed the cathodic reaction to greater extents than the anodic one, especially at low concentration.

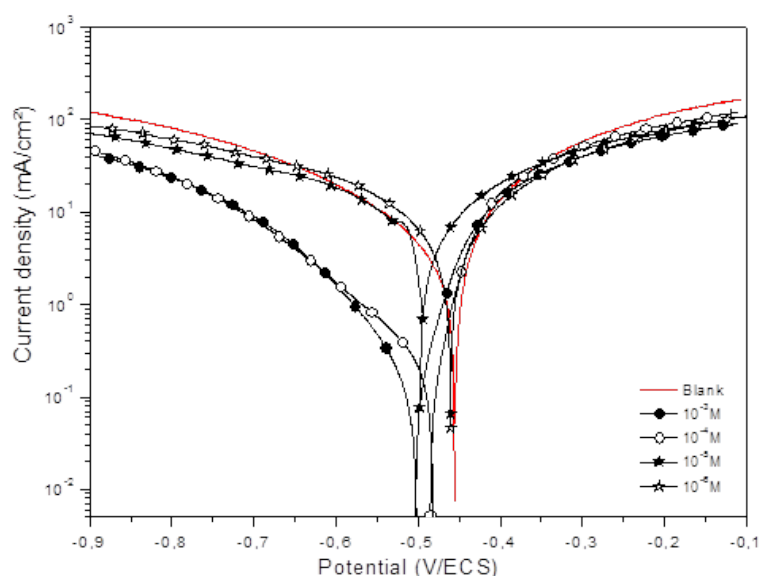


Fig. 3. Polarisation curves for mild steel in 0.5 M H₂SO₄ containing different concentrations of Q-N(CH₃)₂ at 298±2 K

This result suggests that the addition of quinoline derivatives reduces anodic dissolution and also retards the hydrogen evolution reaction. Tafel lines of nearly equal slopes were obtained, indicating that the hydrogen evolution reaction was activation-controlled.

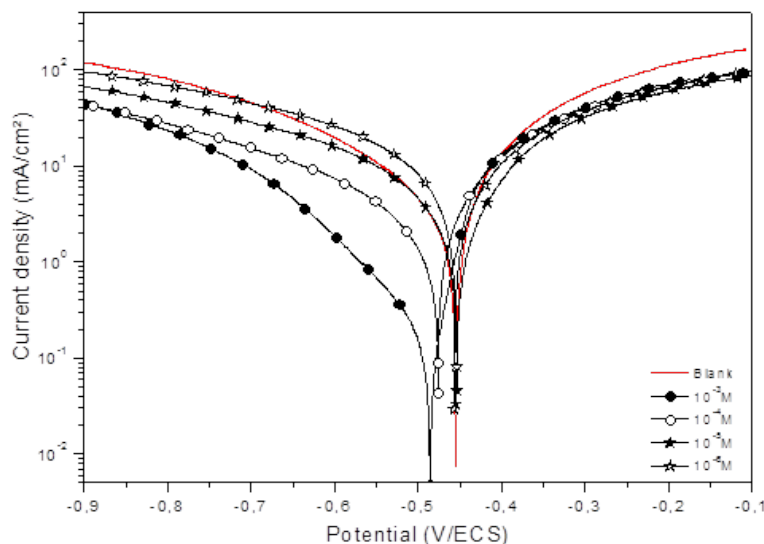


Fig. 4. Polarisation curves for mild steel in 0.5 M H₂SO₄ containing different concentrations of Q-NO₂ at 298±2 K

Values of corrosion current density (I_{corr}) are presented in Table 1. The data show that the I_{corr} values decreased considerably in the presence of Q-N(CH₃)₂ and Q-NO₂ and decreased with increasing inhibitor concentration. No definite trend was observed in the shift of E_{corr} values, in the presence of various concentrations of these inhibitors in 0.5 M H₂SO₄ solutions. In anodic domain, we notice that the presence of Q-N(CH₃)₂ and Q-NO₂ in 0.5 M H₂SO₄ results in a reduction of the anodic current density. This result indicated that these inhibitors exhibited cathodic and anodic inhibition effects.

Therefore Q-N(CH₃)₂ and Q-NO₂ can be classified as inhibitors of relatively mixed effect (anodic/cathodic inhibition) in 0.5 M H₂SO₄.

It is apparent also that the η_{pp} followed the order Q-N(CH₃)₂>Q-NO₂ such as found by the weight loss measurements.

From results given in Table 1, an increase of η (%) with inhibitor concentrations, reaching a maximum value at of 10⁻³ M for both inhibitors, was observed, but better performances were obtained by Q-N(CH₃)₂. We can conclude that the ability of the molecule to chemisorb on the iron surface was dependent on the quinoline substitution. The greater inhibition efficiency may be attributed to the presence of electron donating (-CH₃) group in Q-N(CH₃) compared to electron withdrawing (-NO₂) substituent present in Q-NO₂. These results are comparable with those calculated from weight loss measurements in Table 1 but a little difference can be observed. This observation was also reported by several authors [48,49].

3.2.4. Electrochemical Impedance Spectroscopy (EIS)

The corrosion behaviour of mild steel in 0.5 M H₂SO₄ solution in the absence and presence of quinoline derivatives was also investigated by the electrochemical impedance spectroscopy (EIS) at 298±2 K. Nyquist plots of mild steel in uninhibited and inhibited acidic solutions (0.5 M H₂SO₄) containing various concentrations of Q-N(CH₃)₂ and Q-NO₂ are given in Fig. 5 and 6.

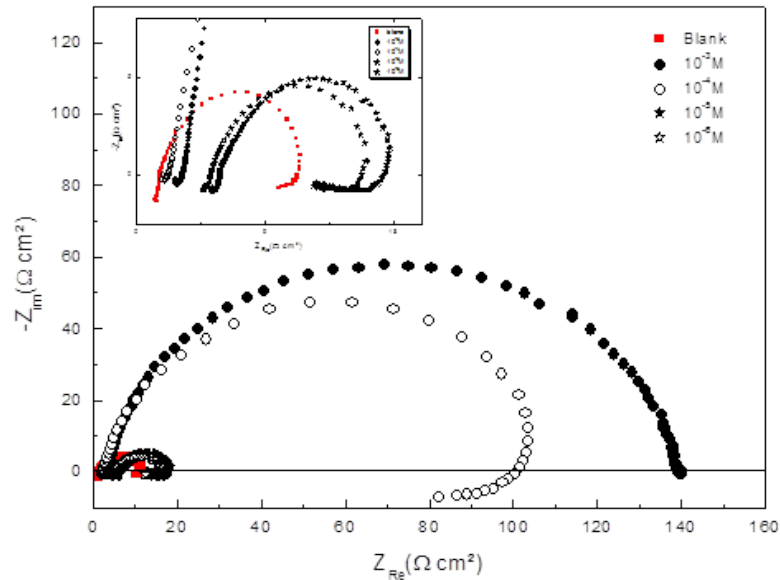


Fig. 5. Nyquist diagrams for mild steel in 0.5 M H₂SO₄ solution in the absence and presence of various concentrations of Q-N(CH₃)₂ at 298±2 K

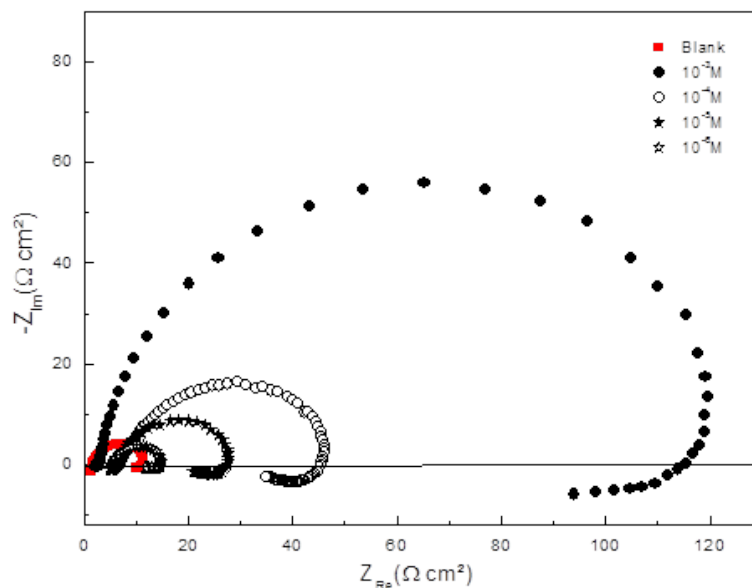


Fig. 6. Nyquist diagrams for mild steel in 0.5 M H₂SO₄ solution in the absence and presence of various concentrations of Q-NO₂ at 298±2 K

The impedance response of mild steel in 0.5 M H₂SO₄ solution was significantly changed after the addition of both inhibitors, and the impedance of the inhibited system increased with inhibitor concentration. Furthermore, at 10⁻³ M concentration of *Q-N(CH₃)₂* and *Q-NO₂* larger diameter semicircles were obtained than the other three lower concentrations of these compounds (Figures 5 and 6). In the presence of these inhibitors, in the completely studied concentration interval, the electrochemical impedance spectra in complex plane depiction of Nyquist diagram show a depressed capacitive loop in the high frequency (HF) range and an inductive loop in the lower frequency (LF) range. The HF capacitive loop can be attributed to the charge transfer reaction and time constant of the electric double layer and to the surface non-homogeneity of interfacial origin, such as those found in adsorption processes on metal surface and the LF inductive loop may be attributed to the relaxation process obtained by adsorption of the species like Cl_{ads}^- and H_{ads}^+ on working electrode surface [50-55]. It may also be attributed to the adsorption of inhibitor on the electrode surface [56] or to the re-dissolution of the passivated surface at low frequencies [57]. In other words, the inductive behaviour at low frequency is probably due to the consequence of the layer stabilization by products of the corrosion reaction on the electrode surface (for example, [FeOH]_{ads} and [FeH]_{ads}) involving inhibitor molecules and their reactive products [58].

The LF inductive loop (10⁻⁶ M, 10⁻⁵ M, 10⁻⁴ M and 10⁻³ M) of *Q-NO₂* and (10⁻⁶ M, 10⁻⁵ M, and 10⁻⁴ M) of *Q-N(CH₃)₂* may be a consequence of the layer stabilization by-products of the corrosion reaction at the electrode involving inhibitor molecules and their reactive products [59].

Table 2. Impedance parameters and inhibition efficiency for mild steel in 0.5 M H₂SO₄ solution without and with different concentration Q-X at 298±2 K

<i>Conc. / M</i>	$R_s / \Omega \text{ cm}^2$	$C_{dl} / \mu\text{F cm}^{-2}$	$R_{ct} / \Omega \text{ cm}^{-2}$	$\eta / \%$
Blank	1.3	244	9	-
Q-N(CH ₃) ₂ / 0.5 M H ₂ SO ₄ / Mild steel				
10 ⁻⁶	4.9	203	16	43.7
10 ⁻⁵	4.0	194	18	50.0
10 ⁻⁴	2.0	106	107	91.5
10 ⁻³	3.5	104	139	93.5
Q-NO ₂ / 0.5 M H ₂ SO ₄ / Mild steel				
10 ⁻⁶	6.3	253	16	43.7
10 ⁻⁵	6.0	203	25	64.0
10 ⁻⁴	6.2	131	42	79.0
10 ⁻³	4.0	91	118	92.3

The LF inductive loop was absent for 10^{-3} M of $Q-N(CH_3)_2$ concentration which may be attributed to the formation of a protective film causing hindrance in the dissolution process [60]. The impedance parameters, such as R_s , R_{ct} , C_{dl} and inhibition efficiency η (%), obtained from fitting the *EIS* data using the equivalent circuits of Figure 7.a and 7.b, are calculated and listed in Table 2.

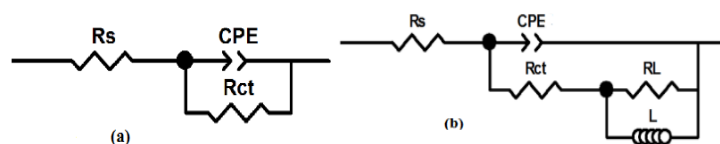


Fig. 7. Equivalent circuit of mild steel in 0.5 M H_2SO_4 (a) without inductive loop. (b) and with inductive loop

The characteristic parameters associated to the impedance diagram (R_t and C_{dl}) and η (%) are given in Table 2. In the case of impedance study, η (%) is calculated using R_t as described elsewhere [61]. η (%) for $Q-N(CH_3)_2$ and $Q-NO_2$ has increased with inhibitor concentration. The inhibition efficiencies, calculated from *Ac* impedance results, show the same trend as those obtained from *dc* polarisation and weight loss measurements. Comparison of the η (%) values obtained using these methods show acceptable agreement. As it can be seen from Table 2, the R_{ct} values increased with the increasing the concentrations of the inhibitors. On the other hand, the values of C_{dl} decreased with an increase in the inhibitors concentration. This situation was the result of an increase the surface coverage by the inhibitor, which led to an increase in the inhibition efficiency (Table 2). The thickness of the protective layer, δ_{org} , was related to C_{dl} by the following equation:

$$\delta_{org} = \varepsilon_0 \cdot \varepsilon_r / C_{dl} \quad (8)$$

where ε_0 is the vacuum dielectric constant and ε_r is the relative dielectric constant.

This decrease in the C_{dl} , which can result from a decrease in local dielectric constant and/or an increase in the thickness of the electrical double layer, suggested that the $Q-N(CH_3)_2$ and $Q-NO_2$ molecules function by adsorption at the metal/solution interface.

Thus, the change in C_{dl} values was caused by to the gradual replacement of water molecules by the adsorption of the organic molecules on the metal surface, decreasing the extent of the metal dissolution [62]. In general, two modes of adsorption can be considered. The proceeding of physical adsorption requires the presence of electrically charged metal surface and charged species in the bulk of the solution. Chemisorption process involves charge sharing or charge transfer from the inhibitor molecules to the metal surface. This is possible in case of positive as well as negative charges on this surface. The presence, with a

transition metal, having vacant, low-energy electron orbital, of an inhibitor molecule having relatively loosely bound electrons or heteroatoms with lone-pair electrons facilitates this adsorption [63,64]. In other hand, the quinolines derivatives which possess two nitrogen atoms with electron-pair donors can accept a proton, leading the cationic forms. These species can be adsorbing by the metal surface because of attractive forces between the negatively charged metal and the positively charged quinolines.

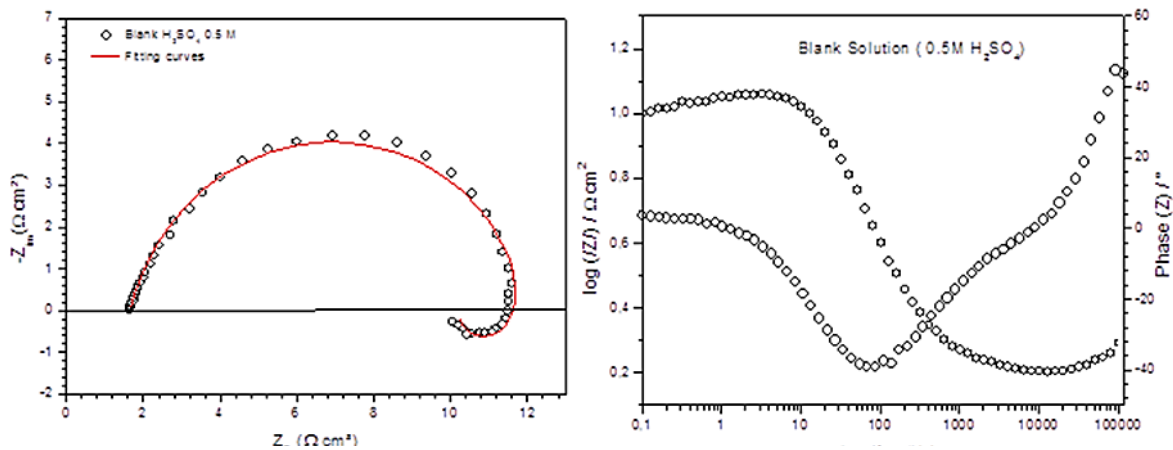


Fig. 8. Nyquist and Bode diagrams ($\log f$ vs. $\log|Z|$) and phase angle ($\log f$ vs. α°) plot of impedance spectra for mild steel in 0.5 M H_2SO_4 at 298 ± 2 K

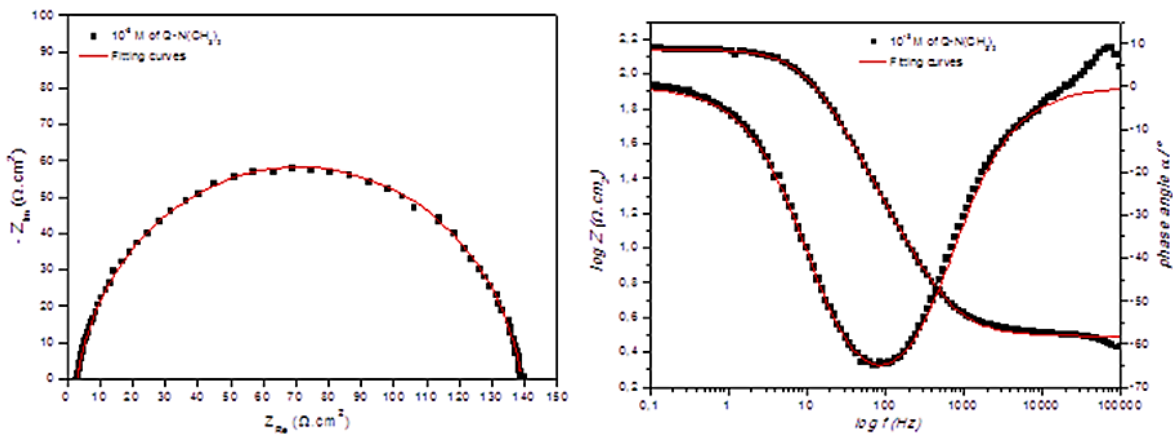


Fig. 9. EIS Nyquist and Bode diagrams ($\log f$ vs. $\log|Z|$) and phase angle ($\log f$ vs. α°) plot of impedance spectra for mild steel / 0.5 M H_2SO_4 / 10^{-3} M Q-N(CH₃)₂ interface: (scater) experimental; (---) fitted data using structural in Fig. 4b

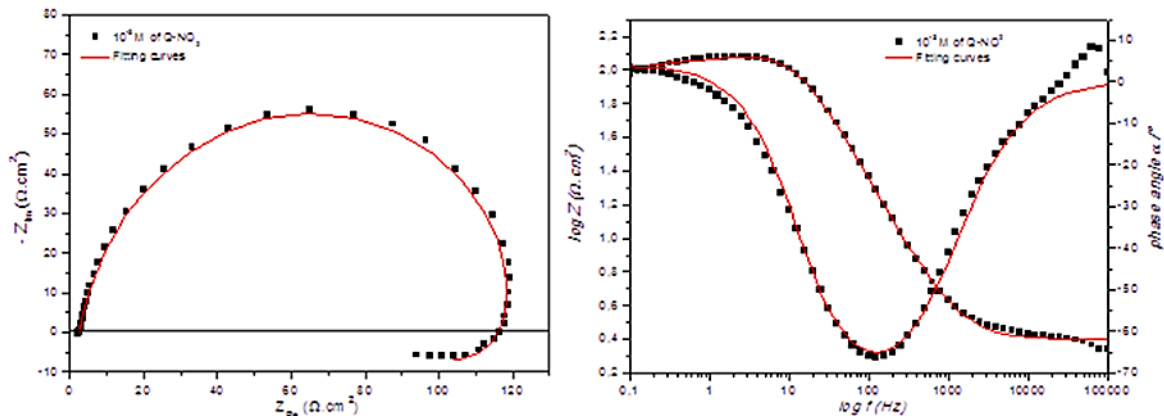


Fig. 10. EIS Nyquist and Bode diagrams ($\log f$ vs. $\log|Z|$) and phase angle ($\log f$ vs. α°) plot of impedance spectra for mild steel/ $0.5 \text{ M H}_2\text{SO}_4/10^{-3} \text{ M Q-NO}_2$ interface: (scater) experimental; (---) fitted data using structural in Fig. 4b

Excellent fit with the model was obtained for all experimental data (Fig. 8, 9 and 10). The Nyquist and Bode plots of both experimental and simulated data of mild steel in $0.5 \text{ M H}_2\text{SO}_4$ solution without and with 10^{-3} M of $\text{Q-(CH}_3)_2$ and Q-NO_2 are shown in Fig. 8, 9 and 10. It is clear that the impedance plots are in accordance with those calculated by the used equivalent circuit model. Various parameters such as charge-transfer resistance (R_{ct}) and double layer capacitance (C_{dl}) obtained from impedance measurements are shown in Table 2, which contains all the impedance parameters obtained from the simulation of experimental impedance data, including R_{ct} .

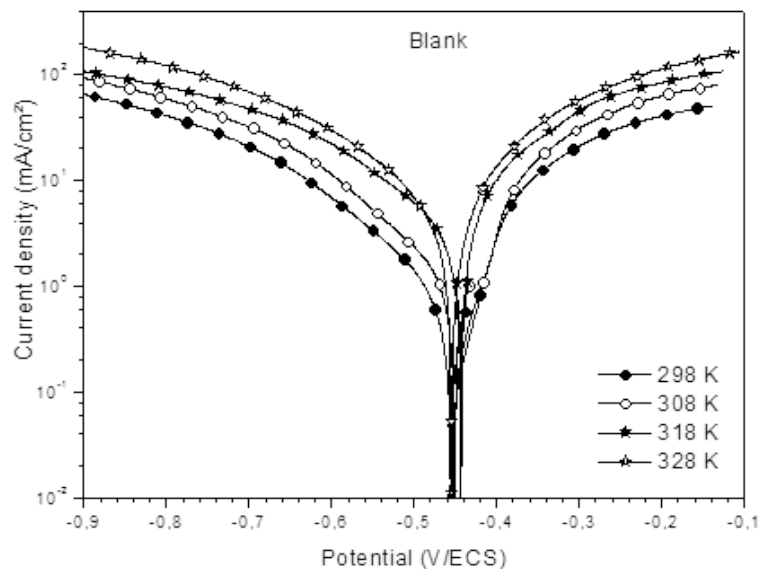


Fig. 11. Potentiodynamic polarization curves for mild steel in $0.5 \text{ M H}_2\text{SO}_4$ at different temperature

3.3. Effect of temperature

The effect temperature on the corrosion inhibition of mild steel 0.5 M H₂SO₄ without and with inhibitors was studied in the temperature range 298 to 328±2 K. Their potentiodynamic polarization is shown in Fig. 11 and 12.

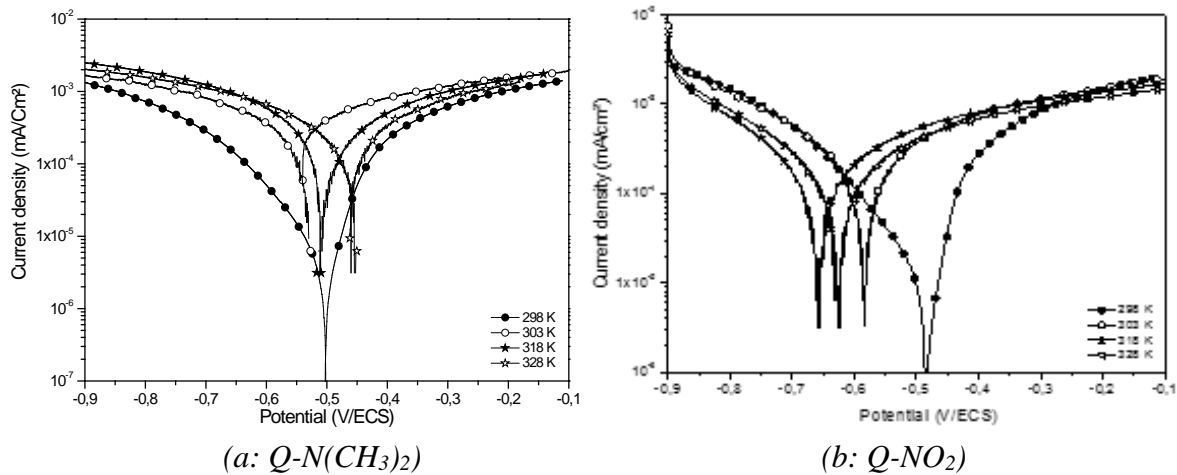


Fig. 12. Potentiodynamic polarization curves for mild steel in 0.5M H₂SO₄ with 10⁻³ of quinoline derivatives at different temperature

Table 3. Electrochemical and activation parameters and the corresponding inhibition efficiencies at various temperature of mild steel in 0.5 M H₂SO₄ in absence and presence of 10⁻³ M of quinoline derivatives

Temperature (K)	E_{corr} (mV/SCE)	i_{corr} (mA cm ⁻²)	η_{PP} (%)	E_a (KJ mol ⁻¹)	ΔH_a (KJ mol ⁻¹)	ΔS_a (J K ⁻¹ mol ⁻¹)
<i>Blank solution (0.5 M H₂SO₄ without inhibitor's)</i>						
298±2	-451	1850	-	15.2	12.5	-28.6
303±2	-453	2250	-	-	-	-
318±2	-449	2480	-	-	-	-
328±2	-442	3340	-	-	-	-
<i>10⁻³ of Q-N(CH₃)₂ / 0.5 M of H₂SO₄</i>						
298±2	-500	118	93.6	45.7	43.1	50.7
303±2	-527	190	91.6	-	-	-
318±2	-507	328	86.8	-	-	-
328±2	-450	644	80.7	-	-	-
<i>10⁻³ of Q-NO₂ / 0.5 M of H₂SO₄</i>						
298±2	-483	154	91.7	37.0	34.5	23.6
303±2	-585	201	91.1	-	-	-
318±2	-628	369	85.1	-	-	-
328±2	-660	577	82.7	-	-	-

Table 3 shows the electrochemical parameters extracted from the potentiodynamic polarization curves of mild steel in 0.5 M H₂SO₄ in the presence of 10⁻³ M of each substituted quinoline compounds. It is clear that the current density values increased and the inhibition efficiency of the studied compounds decreased slightly with increasing of temperature.

However, the logarithm of corrosion rates (Ln *i*_{corr}) versus reciprocal of absolute temperature (1/T) for 0.5 M H₂SO₄ without and with substituted phenyltetrazole was examined (Figure 13) using the Arrhenius equation:

$$\text{Ln } i_{\text{corr}} = -\frac{E_a}{RT} + \text{Ln}A \quad (9)$$

where A is the Arrhenius pre-exponential constant, R is the universal gas constant, *E*_a is the apparent activation energy and T is the absolute temperature. The values obtained from the slope of the linear plots are shown in Table 3.

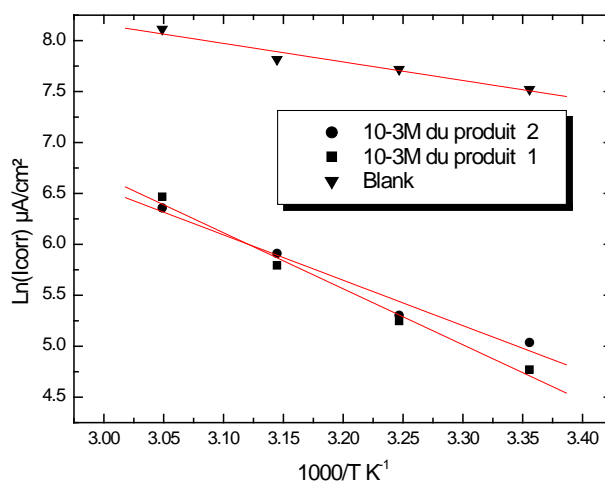


Fig. 13. Arrhenius plots of mild steel in 0.5 M H₂SO₄ without and with 10⁻³ M of different substituted quinoline

It is found that all the linear regression coefficients are close to 1, indicated that the corrosion of mild steel in hydrochloric acid can be explained using the kinetic model. As observed from the Table 3, the *E*_a increased with Q-N(CH₃)₂ addition and decreased in the case of Q-NO₂ addition compared to the uninhibited solution (Blank solution). The increase in *E*_a in the presence of Q-N(CH₃)₂ may be interpreted as physical adsorption. Indeed, a higher energy barrier for the corrosion process in the presence of inhibitors was associated with physical adsorption or weak chemical bonding between the inhibitors species and the mild steel surface [65,66]. Szauer et al. have explained that the increase in *E*_a can be attributed to decrease in the inhibitor adsorption at metallic surface with the rise of temperature [67]. Q-N(CH₃)₂ is an organic base that easily protonates to give a cationic form in acid medium. The *E*_a value was greater than 20 kJ mol⁻¹ in both the presence and absence of inhibitor, which revealed that the entire process was controlled by the surface reaction

[68]. So, the decrease of E_a in the case of Q-NO₂ probably was attributed to chemisorption of these inhibitors molecules on the mild steel surface [69]. In this context, Singh et al. have considered that the increase in temperature caused an increase in the electron density at the adsorption centers, which improved the inhibition efficiency.

The other kinetic parameters such as enthalpy of adsorption (ΔH_a) and entropy of adsorption (ΔS_a) were obtained from transition state equation:

$$\ln \frac{i_{corr}}{T} = \ln \left(\frac{R}{Nh} \right) + \left(\frac{\Delta S_a}{R} \right) - \frac{\Delta H_a}{RT} \quad (10)$$

Where i_{corr} is the corrosion rate, h the Plank's constant and N is Avogadro's number, ΔH_a the enthalpy of activation and ΔS_a the entropy of activation.

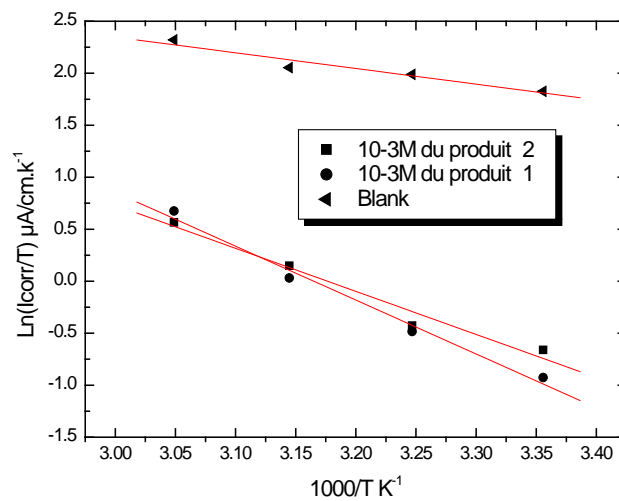


Fig. 14. Transition Arrhenius plots of mild steel in 0.5 M H₂SO₄ without and with 10⁻³ M of different substituted quinoline

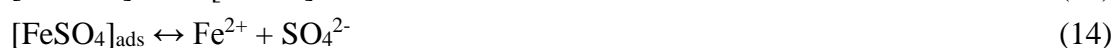
Figure 14 shows the variation of $\ln(i_{corr}/T)$ function ($1/T$) as a straight line with a slope of $(-\Delta H_a/R)$ and the intersection with the y-axis is $[\ln(R/Nh) + (\Delta S_a/R)]$. From these relationships, values of ΔS_a and ΔH_a can be determined. The activation parameters (ΔH_a and ΔS_a) which determined from the slopes of Arrhenius lines without and with inhibitors, are summarized in Table 3. It is seen that the ΔH_a value for dissolution reaction of mild steel in 0.5 M H₂SO₄ in the presence of Q-N(CH₃)₂ is higher than that in the presence Q-NO₂ and the free solution. In addition, the ΔH_a values in the presence Q-NO₂ are lower than that in their absence.

However, the positive values of ΔH_a for both corrosion processes without and with inhibitors reveal the endothermic nature of the mild steel dissolution process and indicate that the dissolution of the mild steel is difficult [70]. The same remarks were observed for the E_a values indicating that the corrosion process must involve a gaseous reaction, simply the hydrogen evolution reaction, associated with a decrease in the total reaction volume [71].

Additionally, Table 3 shows that the ΔS_a values increase with the presence of Q-N(CH₃)₂ compared to blank solution, which mean an increase in disorder during the transition from reactant to the activated complex during corrosion process [72]. Also the ΔS_a values tend to more negative values as the Q-NO₂ addition showing more ordered behaviour leading to increase inhibition efficiency.

3.4. Mechanism of adsorption and inhibition

A clarification of the mechanism of inhibition requires full knowledge of the interaction between the protective organic inhibitor and the metal surface. The corrosion behavior of mild steel in H₂SO₄ solution has received considerable attention in the literature [73,74]. The mechanism of the anodic dissolution of iron is shown in the following equations:



Assumed in presence of SO₄²⁻ ions, reaction (9) rapid proceeds on the metal surface. Hence, the anodic iron dissolution was controlled by both electrodisolution of mild steel and diffusion of soluble [FeSO₄]_{ads} to the bulk solution. As illustrated in Fig. 15, a mechanism has been proposed to explain the adsorption model of inhibitor (Inh) on the mild steel surface. In the low-lying area, sulfate anions are first adsorbed onto the positively charged metal surface. Because quinoline derivatives are organic bases, then Q-N(CH₃)₂ and Q-NO₂ molecules can exist as protonated form (Org.inh,H⁺) in acidic solution.

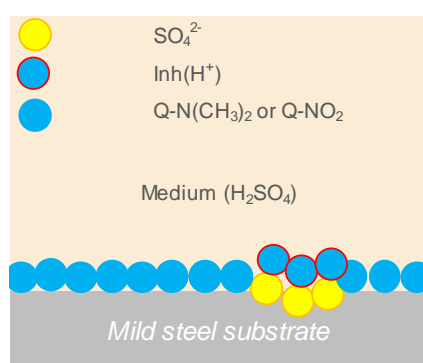


Fig. 15. Proposed mechanism for the adsorption of inhibitor molecules on the mild steel surface in H₂SO₄ medium

Inhibitor quickly reacts with “Fe” and forms a strong protective layer in the non-corroded area. The layer is very thin and is presumably a single monolayer. On the other hand, Inh(H⁺)

reacts with Fe(II) and forms a thick and protective $[\text{FeSO}_4^{2-}, \text{Org.inh}, \text{H}^+]$ complex. Therefore, aggressive ions were obstructed by the protective film and the steel was effectively protected from corrosion. Cathodic chemical process occurs as following: [75]



Then, the protonated inhibitor molecules can be also adsorbed at cathodic sites of mild steel in competition with hydrogen ions that going to reduce to H_2 gas evolution.

3.5. Surface morphology analysis

The surface morphology of mild steel due to corrosion process was confirmed by the SEM images of the polished and corroded mild steel surface in the absence and presence of inhibitors (Figs. 16 and 17).

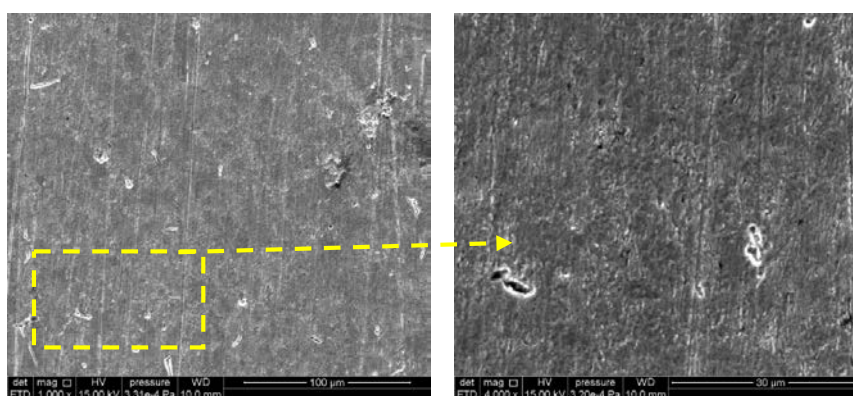


Fig. 16. Surface morphology of mild steel after immersion for 6 h in 0.5 M H_2SO_4 without inhibitor

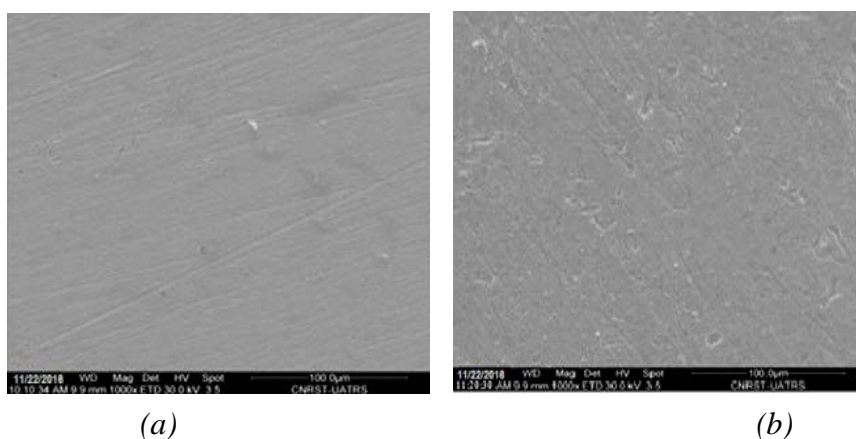


Fig. 17. Surface morphology of mild steel after immersion for 6 h in 0.5 M H_2SO_4 (a) with 10^{-3} M of $\text{Q-N}(\text{CH}_3)_2$ and (b) with 10^{-3} M of Q-NO_2

Fig. 16 represents the SEM image for mild steel surface in 0.5 M H₂SO₄ without inhibitors. It was found that the surface morphologies served as a good indicator of the severity of corrosion attack. However, SEM images of mild steel surface in the presence of inhibitors were observed to be smoother than that of mild surface in 0.5 M H₂SO₄ alone (Figs.17a and 17b).

The influence of the inhibitors addition on the sulfuric acid medium is shown in Fig. 17. The morphology shows a rough surface, characteristic of uniform corrosion of mild steel in acid, that corrosion does not occur in presence of inhibitors and hence corrosion was inhibited strongly when the inhibitors was present in the sulfuric acid solution, and the surface layer is very rough. Also, there is an adsorbed film adsorbed on mild steel surface Fig. 17. In accordance, it might be concluded that the adsorption film can efficiently inhibits the corrosion of mild steel.

4. CONCLUSION

The studied organic compounds Q-N(CH₃)₂ and Q-NO₂ shows excellent inhibition properties for the corrosion of mild steel in 0.5 M H₂SO₄ at 298±2 K, and the corrosion rate of mild steel decreased with increasing the inhibitor's concentration to reach a minimum at 10⁻³ M. However, the inhibition efficiency decrease with temperature of the synthesized inhibitors and the order of inhibition efficiency decreased as follows: Q-N(CH₃)₂ > Q-NO₂. These compounds act as mixed type inhibitors. The results of EIS indicate that the values of C_{dl} tend to decrease and both R_{ct} and η% tends to increase with increasing the inhibitors concentrations. This result can be attributed to an increase of the thickness of the protective film formed on the mild steel surface. These inhibitors were found to obey Langmuir adsorption isotherm. Thermodynamic adsorption parameters (ΔH_a, ΔS_a and ΔG_a) showed that the studied inhibitor was adsorbed on mild steel surface by an endothermic and spontaneous process. Reasonably good agreement was observed between the obtained data from weight loss, potentiodynamic polarization curves and electrochemical impedance spectroscopy techniques. The passive film formed on the metal surface was characterized by SEM.

Acknowledgments

The authors appreciate the experimental support given by all members of "Laboratory of Materials Engineering and Environment: Modeling and Application, Faculty of Science, University Ibn Tofail, Kenitra, Morocco". We are pleased to acknowledge them.

REFERENCES

- [1] Y. El Kacimi, M. A. Azaroual, R. Tourir, M. Galai, K. Alaoui, M. Sfaira, M. Ebn Touhami, and S. Kaya, *Euro-Mediterr J. Environ. Integr.* 2 (2017) 1.
- [2] Y. Abboud, A. Abourriche, T. Saffaj, M. Berrada, M. Charrouf, A. Bennamara, N. Al Himidi, and H. Hannache, *Mater. Chem. Phys.* 105 (2007) 1.
- [3] A. O. James, N. C. Oforka, and K. Abiola, *Int. J. Electrochem. Sci.* 2 (2007) 278.
- [4] K. Alaoui, Y. El Kacimi, M. Galai, K. Dahmani, R. Tourir, A. El Harfi, and M. Ebn Touhami, *Anal. Bioanal. Electrochem.* 8 (2016) 830.
- [5] A. Benabida, M. Galai, M. Cherkaoui, and O. Dagdag, *Anal. Bioanal. Electrochem.* 8 (2016) 962.
- [6] M. Galai, M. Rbaa, Y. El Kacimi, M. Ouakki, N. Dkhirech, R. Tourir, B. Lakhrissi, and M. Ebn Touhami, *Anal. Bioanal. Electrochem.* 9 (2017) 80.
- [7] M. Bouklah, B. Hammouti, A. Aouniti, and T. Benhadda, *Prog. Org. Coat.* 47 (2004) 225.
- [8] M. Rbaa, M. Galai, Y. El Kacimi, M. Ouakki, R. Tourir, B. Lakhrissi, and M. Ebn Touhami, *Portugaliae Electrochim. Acta* 35 (2017) 323.
- [9] M. Galai, M. El Gouri, O. Dagdag, Y. El Kacimi, A. Elharfi, and M. Ebn Touhami, *J. Mater. Environ. Sci.* 7 (2016) 1562.
- [10] S. Muralidhan, K. L. N. Phani, S. Pitchumani, and S. V. K. Iyer, *J. Electrochem. Soc.* 142 (1995) 1478.
- [11] C. Verma, M. A. Quraishi, and Ain Shams, *J. Phys. Chem. C* 120 (2016) 11598.
- [12] Y. El Kacimi, R. Tourir, M. Galai, R. A. Belakhmima, A. Zarrouk, K. Alaoui, M. Harcharras, H. El Kafssaoui, and M. Ebn Touhami, *J. Mater. Environ. Sci.* 7 (2016) 371.
- [13] R. B. N. Baig and R. S. Varma, *Chem. Soc. Rev.* 41 (2012) 1559.
- [14] B. Hammouti, A. Aouniti, M. Taleb, M. Brighli, and S. Kertit, *Corrosion* 51 (1995) 411.
- [15] A. Aouniti, B. Hammouti, S. Kertit, and M. Brighli, *Bull. Electrochem.* 14 (1998) 193.
- [16] A. El-Ouafi, B. Hammouti, H. Oudda, S. Kertit, R. Touzani, and A. Ramdani, *Anti-Corros. Meth. Mater.* 49 (2002) 199.
- [17] S. Kertit, K. Bekkouch, M. El-Farissi, A. Aouniti, and B. Hammouti, in: *Proc. Int. Conf. Corros., Concorn 97, Mumbai, India (1997)* pp. 672.
- [18] R. Salghi, L. Bazzi, B. Hammouti, A. Bouchart, S. Kertit, Z. A. Ait Addi, and Z. EL Alami, *Ann. Chim. Sci. Mat.* 25 (2000) 187.
- [19] F. Bentiss, M. Traisnel, L. Gengembre, and M. Lagrene´e, *Appl. Surf. Sci.* 161 (2000) 194.
- [20] F. Bentiss, M. Lagrene´e, M. Traisnel, and J. C. Hornez, *Corros. Sci.* 41 (1999) 789.

- [21] F. Bentiss, M. Traisnel, L. Gengembre, and M. Lagrene´e, *Appl. Surf. Sci.* 152 (1999) 237.
- [22] F. Bentiss, M. Lagrene´e, B. Mehdi, B. Mernari, M. Traisnel, and H. Vezin, *Corrosion* 58 (2002) 399.
- [23] S. Kertit, and B. Hammouti, *Appl. Surf. Sci.* 93 (1996) 59.
- [24] S. Kertit, H. Essouffi, B. Hammouti, and M. Benkaddour, *J. Chim. Phys.* 95 (1998) 2072.
- [25] Y. Elkacimi, M. Achnin, Y. Aouine, M. EbnTouhami, A. Alami, R. Tourir, M. Sfaira, D. Chebabe, A. Elachqar, and B. Hammouti, *Portugaliae Electrochim. Acta* 30 (2012) 53.
- [26] M. Galai, M. El Faydy, Y. El Kacimi, K. Dahmani, K. Alaoui, R. Tourir, B. Lakhrissi, and M. Ebn Touhami, *Portugaliae Electrochim. Acta* 35 (2017) 233.
- [27] M. Rbaa, M. Galai, M. EL Faydy, Y. El Kacimi, M. Ebn Touhami, A. Zarrouk, and B. Lakhrissi, *J. Mater. Environ. Sci.* 8 (2017) 3529.
- [28] A. Dafali, B. Hammouti, A. Aouniti, R. Mokhlisse, S. kertit, and K. El-kacemi, *Ann. Chim. Sci. Mat.* 25 (2000) 437.
- [29] A. Dafali, B. Hammouti, and S. Kertit, *J. Electrochem. Soc. Ind.* 50 (2001) 62.
- [30] G. K. Gomma, and M. H. Wahdan, *Mater. Chem. Phys.* 47 (1997) 176.
- [31] F. Bentiss, M. Traisnel, H. Vezin, and M. Lagrene´e, *Corros. Sci.* 45 (2003) 371.
- [32] M. Lagrene´e, B. Mernari, N. Chaibi, M. Traisnel, H. Vezin, and F. Bentiss, *Corros. Sci.* 43 (2001) 951.
- [33] F. Bentiss, M. Traisnel, and M. Lagrene´e, *Corros. Sci.* 42 (2000) 127.
- [34] F. Bentiss, M. Lagrene´e, M. Traisnel, and J. C. Hornez, *Corrosion* 55 (1999) 968.
- [35] M. M. Osman, *Anti-Corros. Meth. Mater.* 45 (1998) 176.
- [36] W. Durnie, R. D. Marco, A. Jefferson, and B. Kinsella, *J. Electrochem. Soc.* 146 (1999) 1751.
- [37] L. B. Tang, G. N. Mu, and G. H. Liu, *Corros. Sci.* 45 (2003) 2251.
- [38] T. P. Zhao, and G. N. Mu, *Corros. Sci.* 41 (1999) 1937.
- [39] M. H. Wahdan, *Mater. Chem. Phys.* 49 (1997) 135.
- [40] A. Chetouani, A. Aounti, B. Hammouti, N. Benchat, T. Benhadda, and S. Kertit, *Corros. Sci.* 45 (2003) 1675.
- [41] M. H. Wahdan, *Mater. Chem. Phys.* 49 (1997) 135.
- [42] L. Feng, X. Wang, and Z. Chen, *Spectrochim. Acta Part A* 71 (2008) 312.
- [43] M. S. AbdelAal, S. Radwan, and A. El Saied, *Br. Corros. J.* 18 (1983) 2.
- [44] T. Murakawa, and N. Hackerman, *Corros. Sci.* 4 (1964) 387.
- [45] K. D. Allabergenov, and F. K. Kurbanov, *Zashch Met* 15 (1979) 472.
- [46] S. Rengamati, S. Muralidharan, M. Anbu Kulandainathan, and S. Venkatakrishna Iyer, *J. Appl. Electrochem.* 24 (1994) 355.

- [47] J. O. M. Bockris, and B. Yang, *J. Electrochem. Soc.* 135 (1991) 2237.
- [48] N. Hackerman, R. N. Hurd, and R. R. Annand, *Corrosion* 8 (1962) 37.
- [49] G. Oskes, and J. M. Vest, *Br. Corros. J.* 4 (1969) 6617.
- [50] M. A. Amin, S. S. Abd El-Rehim, E. F. El-Sherbini, and R. S. Bayyomi, *Electrochim. Acta* 52 (2007) 3588.
- [51] H. J. W. Lenderink, M. V. D. Linden, and J. H. W. De Wit, *Electrochim. Acta* 38 (1993) 1989.
- [52] M. A. Amin, K. F. Khaled, Q. Mohsen, and H. A. Arida, *Corros. Sci.* 52 (2010) 1684.
- [53] M. Kedam, O. R. Mattos, and H. Takenouti, *J. Electrochem. Soc.* 128 (1981) 257.
- [54] M. A. Veloz, and I. Gonzalez, *Electrochim. Acta* 48 (2002) 135.
- [55] M. Lebrini, F. Robert, A. Lecante, and C. Roos, *Corros. Sci.* 53 (2011) 687.
- [56] K. Alaoui, Y. El Kacimi, M. Galai, R. Touir, K. Dahmani, A. Harfi, and M. Ebn Touhami, *J. Mater. Environ. Sci.* 7 (2016) 2389.
- [57] E. M. Sherif, and S. M. Park, *Electrochim. Acta* 51 (2006) 1313.
- [58] E. J. Kelly, *J. Electrochem. Soc.* 112 (1965) 125.
- [59] Y. Lin, A. Singh, E. E. Ebenso, Y. Wu, C. Zhu, H. Zhu, and J. Tai, *Inst. Chem. Eng.* 46 (2015) 214.
- [60] A. Tazouti, M. Galai, R. Touir, M. Ebn Touhami, A. Zarrouk, Y. Ramli, M. Saraçoğlu, S. Kaya, F. Kandemirli, and C. Kaya, *J. Mol. Liq.* 221 (2016) 815.
- [61] A. K. Singh, and M. A. Quraishi, *Corros. Sci.* 52 (2010) 1373.
- [62] M. Lagrenee, B. Mernari, M. Bouanis, M. Traisnel, and F. Bentiss, *Corr. Sci.* 44 (2002) 573.
- [63] A. H. Mehaute, and G. Grepý, *Solid State Ionics* 9–10 (1989) 17.
- [64] G. Reinhard, and U. Rammet, *Proceedings 6th European Symposium on Corrosion Inhibitors*, Ann. University, Ferrara, (1985) pp. 831.
- [65] M. Stern, and A. L. Geary, *J. Electrochem. Soc.* 104 (1957) 56.
- [66] M. S. Abdelaal, S. Radwan, and A. El Saied, *Br. Corros. J.* 18 (1983) 82.
- [67] W. Peters, *Chemotherapy and Drug Resistance in Malaria*, Academic Press London, New York (1970).
- [68] L. Herrag, B. Hammouti, S. Elkadiri, A. Aouniti, C. Jama, H. Vezin, and F. Bentiss, *Corros. Sci.* 52 (2010) 3042.
- [69] C. S. Venkatachalam, S. R. Rajagopalan, and M. V. C. Sastry, *Electrochim Acta* 26 (1981) 1219.
- [70] H. Gerengi, K. Darowicki, G. Bereket, and P. Slepiski, *Corros. Sci.* 51 (2009) 2573.
- [71] E. A. Noor, *Int. J. Electrochem. Sci.* 2 (2007) 996.
- [72] A. K. Singh, and M. A. Quraishi, *Corros. Sci.* 53 (2011) 1288.
- [73] A. Doner, R. Solmaz, M. Ozcan, and G. Kardas, *Corros. Sci.* 53 (2011) 2902.

- [74] A. Y. Musa, A. A. H. Kadhum, A. B. Mohamad, and M. S. Takriff, *Mater. Chem. Phys.* 129 (2011) 660.
- [75] L. Guo, S. Zhu, S. Zhang, Q. He, and W. Li, *Corros. Sci.* 87 (2014) 366.